Phonon dispersion and quantization tuning of strained carbon nanotubes for flexible electronics

Pierre Gautreau,[1] Tarek Ragab,[1,2] Yanbiao Chu,[1] and Cemal Basaran[1]
[1]*Electronic Packaging Laboratory, State University of New York at Buffalo, 102 Ketter Hall, Buffalo, New York 14260, USA*
[2]*Nanotechnology Research Laboratory, University of Tabuk, Tabuk, 71491, Saudi Arabia and Faculty of Engineering, Alexandria University, Alexandria 21526, Egypt*

(Received 1 April 2014; accepted 10 June 2014; published online 23 June 2014)

Graphene and carbon nanotubes are materials with large potentials for applications in flexible electronics. Such devices require a high level of sustainable strain and an understanding of the materials electrical properties under strain. Using supercell theory in conjunction with a comprehensive molecular mechanics model, the full band phonon dispersion of carbon nanotubes under uniaxial strain is studied. The results suggest an overall phonon softening and open up the possibility of phonon quantization tuning with uniaxial strain. The change in phonon quantization and the resulting increase in electron-phonon and phonon-phonon scattering rates offer further explanation and theoretical basis to the experimental observation of electrical properties degradation for carbon nanotubes under uniaxial strain. © *2014 AIP Publishing LLC*.
[http://dx.doi.org/10.1063/1.4884613]

I. INTRODUCTION

Carbon nanotubes (CNTs) and graphene offer exceptional promise for the next generation of electronic devices, due to their combined impressive electrical,[1] thermal,[2,3] and mechanical[4,5] properties. CNTs have been reported to sustain current densities[1] as high as 10^9 A/cm^2 and failure strains as high as 35%.[5] This combination makes CNTs and graphene prime candidates for base materials in flexible electronic devices.[6–12] Several groups have reported the influence of strain on the energy dispersion relation.[13,14] Ito *et al.*[13] report band gap variations as wide as 1 eV for a 10% change in uniaxial strain in semiconducting CNTs. In Ref. 14, similar variations in the band gap and electronic density of states (DOS) are also reported. The influence of strain on phonon behavior has, however, not been studied in such detail. Experimental results have shown softening of specific phonon modes for graphene under strain.[15] Phonon dispersion calculations for the complete spectrum of phonons in CNTs under uniaxial strain still need to be calculated. Full band calculations of strained phonon dispersion for CNTs are necessary for the simulation and design of CNT and graphene based structures under mechanical strain such as flexible electronic devices. Electron-phonon and phonon-phonon scattering rates used in transport calculations and CNT simulations[16–21] both require knowledge of these dispersions. The electrical properties of CNTs under strain have been shown to deteriorate rather quickly.[22] It has been shown that the conductance of CNTs dramatically reduce in the presence of strain.[23] Tombler *et al.*[23] attribute this drop in conductance to a change in the interatomic bonding from sp2 hybrid bonds to sp3 bonds, which lacks the delocalized π-bond responsible for most of the conduction in CNTs.

In this study, further explanations for the deterioration of electrical properties are taken under consideration through calculations of the influence of strain on the phonon dispersion. In the following sections, supercell theory and a robust molecular mechanics model are used to obtain the strained phonon dispersion in Section II, and study the change in the phonon quantization of CNTs in Section III.

II. METHODOLOGY

In order to find the phonon dispersion relation of graphene, a Laplace transform of time and a discrete Fourier transform of the lattice equation of motion in real space given by Eq. (1), yields Eq. (2) in the frequency and wave-vector domain

$$[M]\{\ddot{u}(t)\} = \sum_{n'=1}^{N}[K_{n-n'}]\{u'_n(t) - u_n(t)\}, \tag{1}$$

$$(\omega^2(\vec{q})[M] + [\hat{K}(\vec{q})])\hat{u}(\vec{q},\omega) = 0, \tag{2}$$

where [M] is the mass matrix, $\ddot{u}_n(t)$ and $u_n(t)$ are the time-dependent acceleration and displacement of atom, respectively, $[K_{n-n'}]$ is the stiffness matrix, $\omega(\vec{q})$ is the frequency of the phonon mode, and $[\hat{K}(\vec{q})]$ is the discrete Fourier transform of the stiffness matrix given as

$$[\hat{K}(\vec{q})] = \sum_{n=0}^{N}[K_{n-0}]e^{-i\vec{q}.\vec{r}_n}, \tag{3}$$

where $\vec{r}_n$ is the position vector of atom n. In order to calculate each stiffness matrix $[K_{n-n'}]$, supercell theory[24–26] is used. The supercell for graphene constructed with fourth neighbor interactions is presented in Fig. 1.

Molecular mechanics is then used to obtain the stiffness matrix for a graphene lattice large enough to have several base unit cells in all directions around the supercell to avoid the effect of the boundary conditions on the atoms composing the supercell (3 nm by 3 nm in this study). The inter-atomic

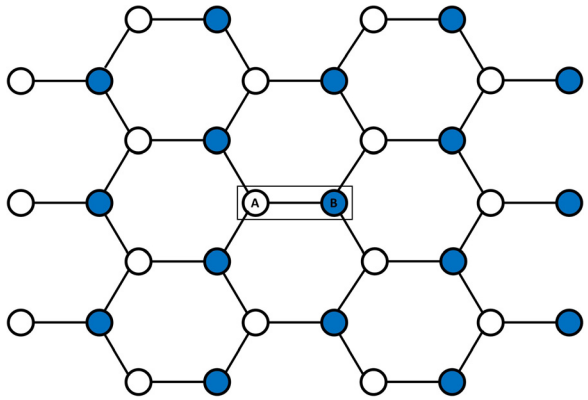

FIG. 1. Supercell for graphene utilizing fourth nearest neighbor interactions.

potential used in the molecular mechanics model is the carbon specific REBO (Reactive Empirical Bond Order) potential.[27] The REBO potential is a pair-wise additive potential, which is capable of modeling the interaction between atoms up to the fourth nearest neighbors through the dihedral conjugation terms.[27] Contrary to the widely used force constant model used for obtaining the phonon dispersion relation,[28] the REBO potential is also capable of fully capturing the non-linear behavior of the interatomic forces. In order to compute the components of the stiffness matrices, the following procedure is used. The lattice is first stretched from two opposite sides of the simulated graphene sheet until the appropriate strain level is reached (2.5%, 5%, 10%, 15%, 20%, and 25%) through a series of applied prescribed displacement increments on the terminal atoms.[29] The system is then allowed to reach equilibrium. Once at equilibrium, each atom in the supercell is moved (one-by-one) by a displacement unit in the x-direction, y-direction, and z-direction. After each move, the resulting force on the atoms of the primary cell (boxed unit cell in Fig. 1) is recorded. Once an atom is moved in a given direction and the force in all three directions has been recorded, the atom is moved back to its original position. This procedure is repeated until all the elements of the stiffness matrix in the space domain have been obtained and then transferred to the wavevector space through Eq. (3). The phonon dispersion is then obtained by computing the eigenvalues of the strained system. The well established zone folding technique[30–34] is then used to compute the phonon dispersion for CNTs.

III. RESULTS

The phonon dispersion relation between the Γ and *M* symmetry points of graphene is presented in Fig. 2 for uniaxial strain of 5%, 15%, and 25%. The effect of strain on the dispersion relation of graphene results in a softening of most of the phonon modes (ZA, ZO, LA, LO, and TO). This is, however, not entirely the case for the transverse accoustic (TA) mode. It appears that, as the uniaxial strain is increased up to about 10%–15%, the TA mode becomes stiffer and results in an increased phonon energy for that mode. For larger strain values, the TA mode does eventually soften. This behavior is to be expected for the TA mode which represents vibrations orthogonal to the direction of the applied

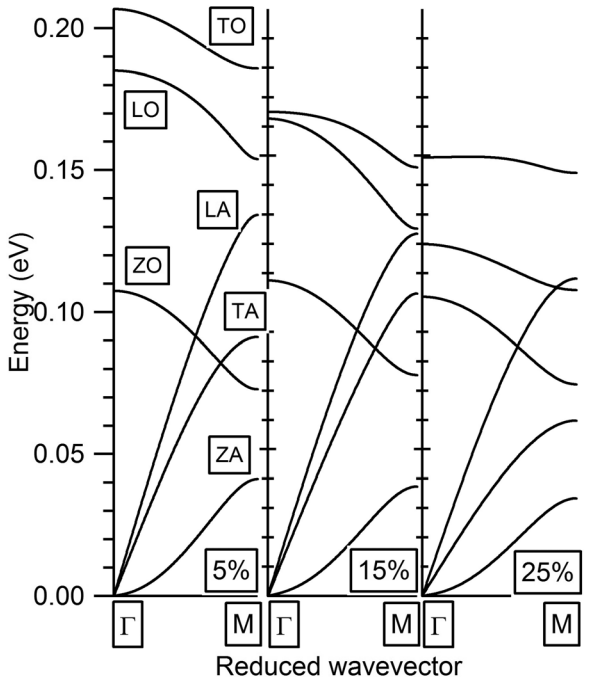

FIG. 2. Phonon dispersion of graphene under 5%, 15%, and 25% uniaxial strain.

strain. As the graphene sheet is stretched in the x-y plane, atomic motion perpendicular to the strain direction requires more energy, until the interatomic spacing becomes large enough that the fourth neighbors interactions become negligible, which results in phonon mode softening for larger strain values. The phonon dispersions for a strained (10,10) metallic armchair CNT obtained with the zone folding method are presented in Figs. 3–7 for strains of 2.5%, 5%, 10%, 15%, and 20%. The (10,10) chirality was chosen because it was shown in Ref. 14 that (10,10) CNTs remain metallic under uniaxial strain, which removes possible electrical property degradation directly from the effect of strain

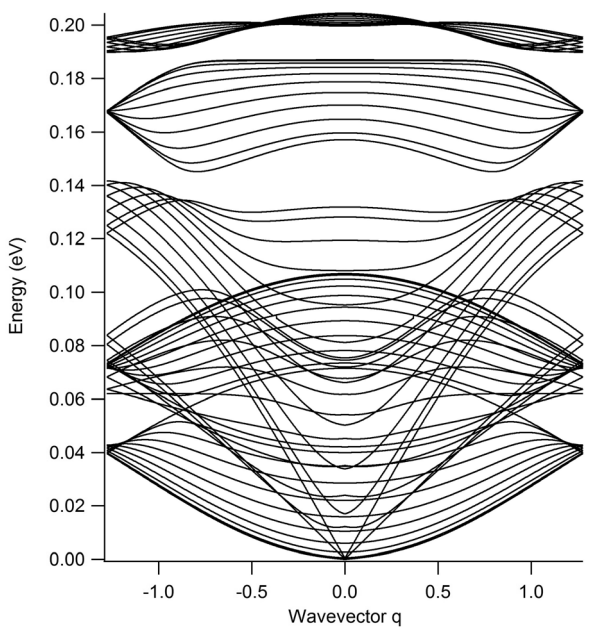

FIG. 3. Phonon dispersion of a (10,10) CNT under 2.5% uniaxial strain.

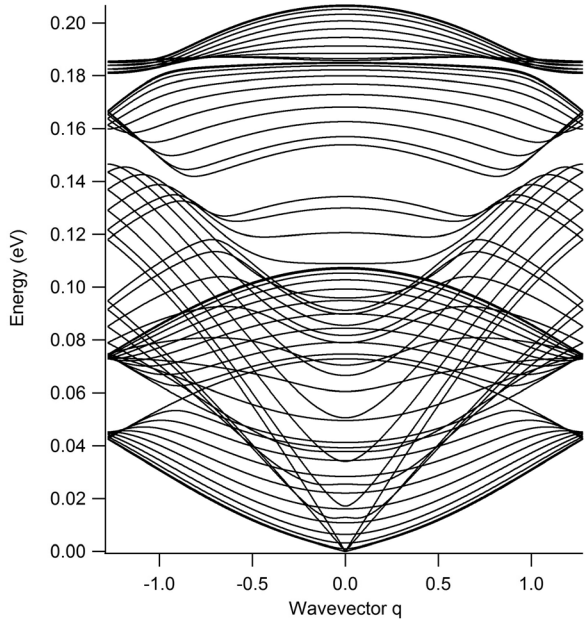

FIG. 4. Phonon dispersion of a (10,10) CNT under 5% uniaxial strain.

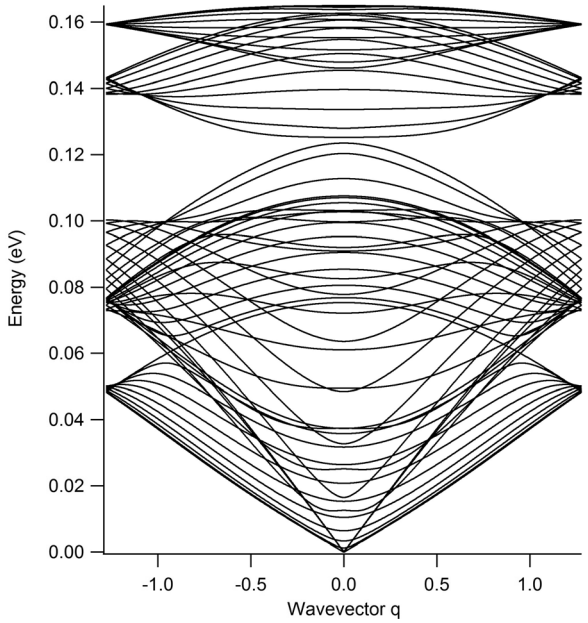

FIG. 6. Phonon dispersion of a (10,10) CNT under 15% uniaxial strain.

on the energy dispersion. In order to quantify the effect of uniaxial strain on the six phonon modes of the (10,10) CNT, the average vibrational energy of each mode is presented in Fig. 8. For the longitudinal modes LA and LO, the effect of uniaxial strain creates an overall downshift of the phonon energy, which is consistent with the phonon softening reported by experimental Raman scattering results.[15] On average, the vibrational energy of LA and LO phonons is lowered by 1.43 meV/% and 2.2 meV/%, respectively. The TO mode also experiences a softening of 2.1 meV/% under uniaxial strain. As expected from the graphene results of Fig. 2, the TA mode experiences a stiffening of 0.75 meV/% up to 10%, followed by a softening of 0.82 meV/%. The behavior of the TA phonons is similar to what occurs in graphene, where the motion transverse to the applied strain is made more difficult in the small strain region until the inter-atomic spacing becomes large enough and the bonding energy is weakened. One significant difference is, however, noted for TA phonons in CNTs. The ring geometry of CNTs provides additional stiffness to these phonons, which prevents the TA phonon energy from downshifting as dramatically as for graphene for large strains. For out-of-plane transverse modes, ZA and ZO, the results suggest that the effect of uniaxial strain on the average vibrational energy is limited. The longitudinal phonons play a major role in the transport behavior of CNTs, and are responsible for most of the electron-phonon scattering events.[5,17,19,21,35] The electron-phonon scattering theory developed by Pennington and Goldsman[21]

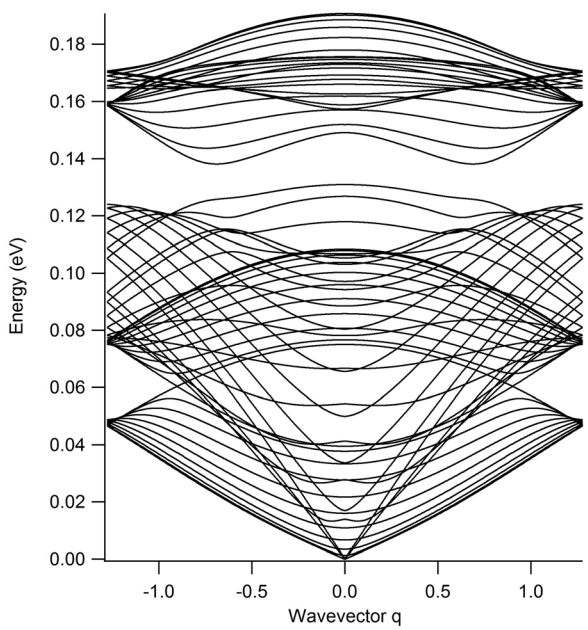

FIG. 5. Phonon dispersion of a (10,10) CNT under 10% uniaxial strain.

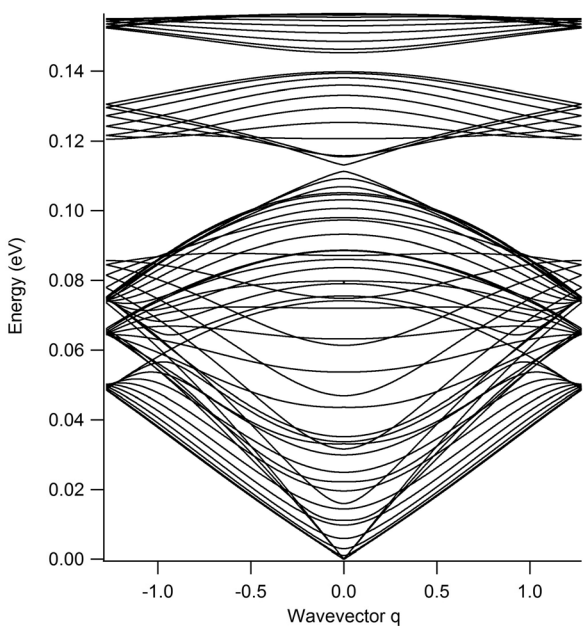

FIG. 7. Phonon dispersion of a (10,10) CNT under 20% uniaxial strain.

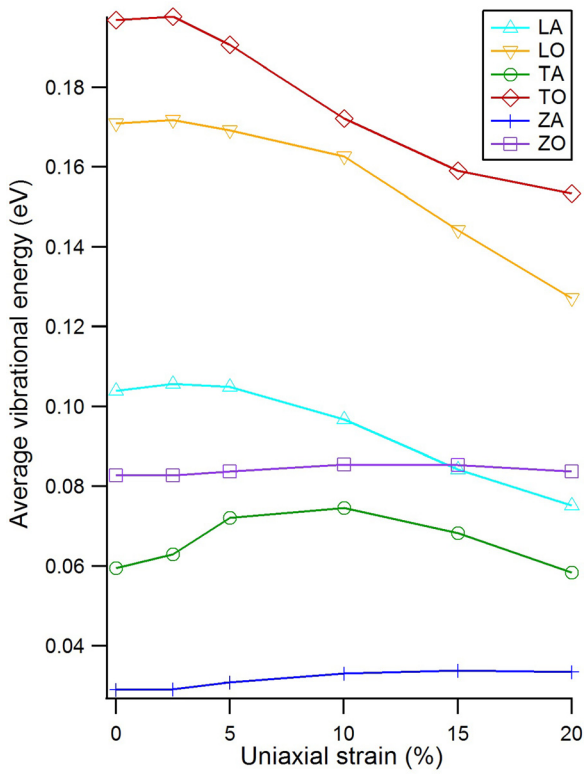

FIG. 8. Average vibrational energy of the phonon modes of a (10,10) CNT.

shows that the scattering rates are inversely proportional to the phonon energy, which means that a change in the phonon quantization and, in particular, the overall longitudinal phonon softening suggested by the results in Figs. 9 and 10 would imply an increase in the electron-phonon scattering rates in CNTs. An increase in the electron-phonon scattering

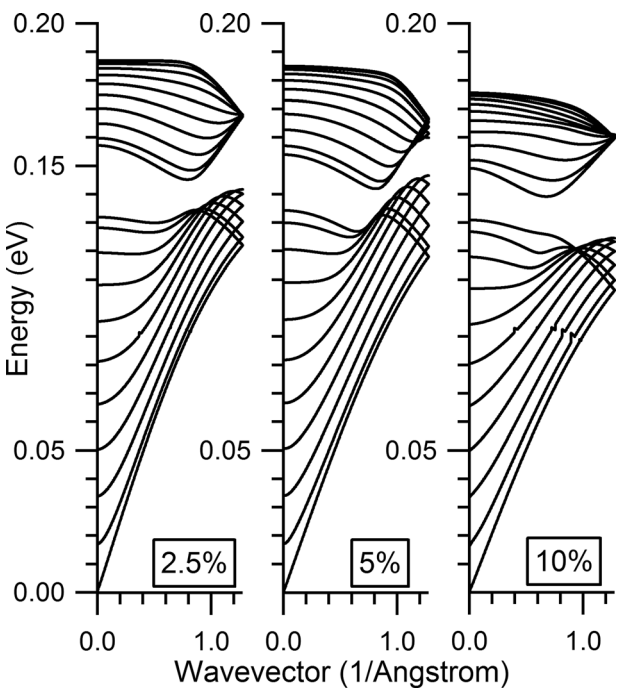

FIG. 9. Phonon dispersion of LA (lower curves) and LO (upper curves) modes for a (10,10) CNT under 2.5%, 5%, and 10% uniaxial strain.

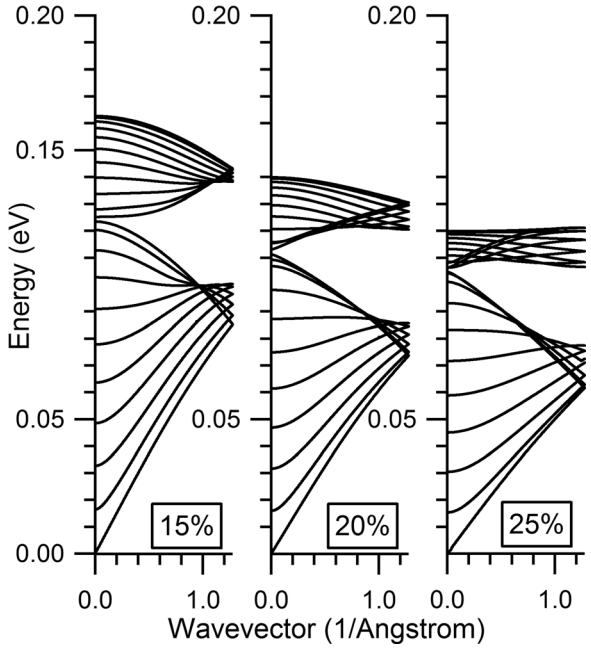

FIG. 10. Phonon dispersion of LA (lower curves) and LO (upper curves) modes for a (10,10) CNT under 15%, 20%, and 25% uniaxial strain.

rates would result in degradation of the electrical conductivity of CNTs, and may provide an alternative explanation to the drop in conductance observed by Tombler *et al.*[23] and the increase in electrical resistance reported by Lu *et al.* and Hoon-Sik *et al.*[36,37] In addition to a change in the electron-phonon coupling, the changes in the phonon dispersion also affect phonon-phonon scattering rates and the associated thermal conductivity of CNTs. Phonon-phonon scattering rates are directly influenced by the phonon energy, phonon-phonon strength of interaction, and phonon density of states. According to Srivastava's phonon-phonon scattering rate formalism,[38,39] an increase in the phonon density of states results in a direct increase in the phonon-phonon scattering rates as described by the following equation:

$$\frac{1}{\tau_{qs}} = \frac{\pi\hbar^2}{144 * m_c^3 (N_o\Omega)^3 \omega(qs)(n_{qs}+1)} \times \sum_{q's',q''s''} \left[\frac{\Phi^2 n_{q's'}(n_{q''s''}+1)\rho\delta_{G,q+q'-q''}}{\omega(q's')\omega(q''s'')} + \frac{1}{2}\frac{\Phi^2 (n_{q's'}+1)(n_{q''s''}+1)\rho\delta_{G,q-q'-q''}}{\omega(q's')\omega(q''s'')} \right], \quad (4)$$

where $N_o\Omega$ is the volume of the CNT lattice, m_c is the mass of a carbon atom, n_{qs} is the phonon occupation number of a phonon with wavevector q and polarization s, ω is the phonon frequency, Φ is the phonon-phonon strength of interaction, and ρ is the phonon density of states (pDOS). The pDOS of LA (LO) phonons are presented in Figs. 11(13) and 12(14) for uniaxial strain from 0% to 20%. The presence of uniaxial strain initially decreases the pDOS of LA phonons for strain values up to 5%, followed by a increase in the pDOS for higher strain. For LO phonons, the results suggest a more uniform increase of the pDOS as the uniaxial strain

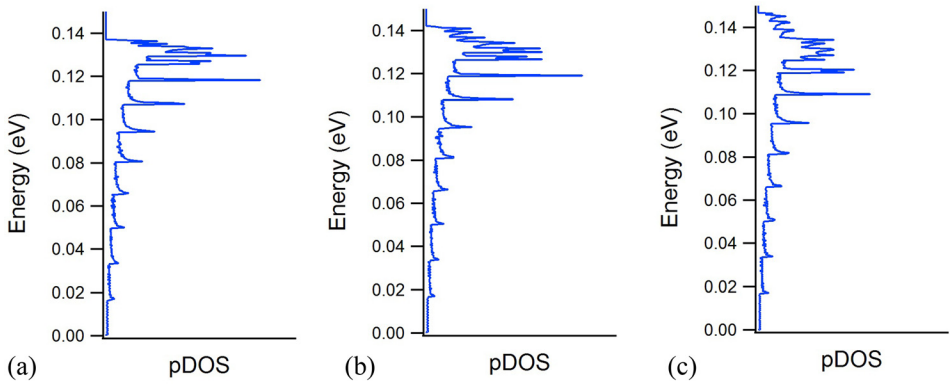

FIG. 11. LA phonon density of states for a (10,10) CNT a) 0% uniaxial strain, b) 2.5% uniaxial strain and c) 5% uniaxial strain.

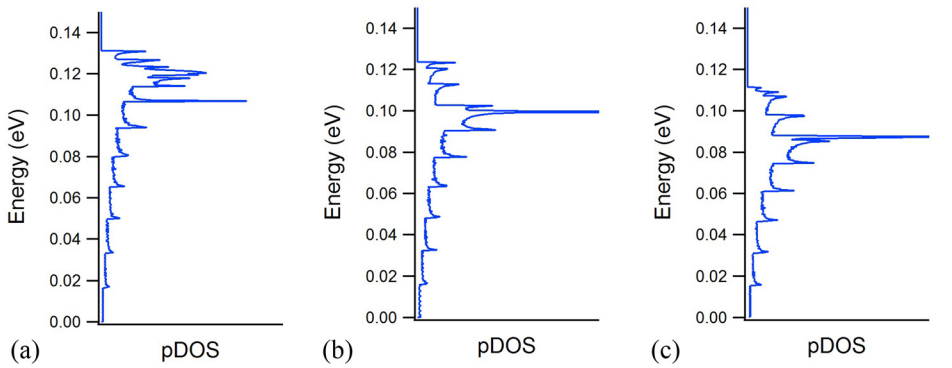

FIG. 12. LA phonon density of states for a (10,10) CNT a) 10% uniaxial strain, b) 15% uniaxial strain and c) 20% uniaxial strain.

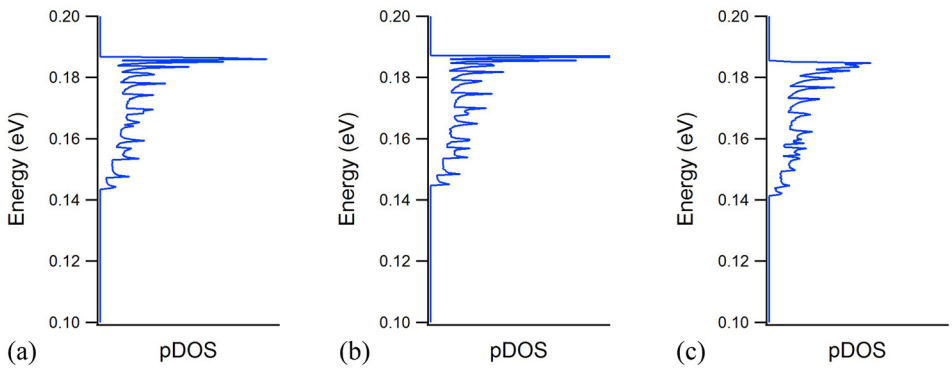

FIG. 13. LO phonon density of states for a (10,10) CNT a) 0% uniaxial strain, b) 2.5% uniaxial strain and c) 5% uniaxial strain.

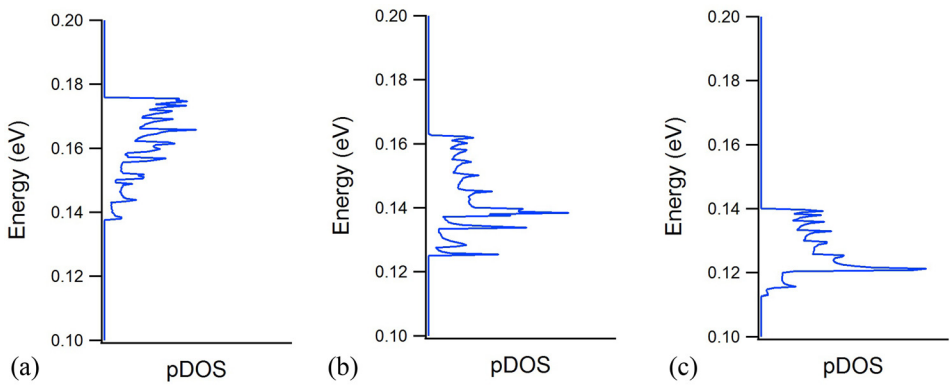

FIG. 14. LO phonon density of states for a (10,10) CNT a) 10% uniaxial strain, b) 15% uniaxial strain and c) 20% uniaxial strain.

increases. In addition to the variation caused by the pDOS, the phonon-phonon scattering rates appear to behave similarly to phonon-electron scattering rates with regards to phonon energy. The overall decrease in phonon energy with strain, shown in Fig. 8, will result in an increase of the phonon-phonon scattering rates. The phonon-phonon strength of interaction term, Φ, is dependent on the third order and above derivatives of the bonding potential, which vary depending on the phonon modes interacting. It is not clear at this point if strain will result in an increase or

decrease of the phonon-phonon scattering rates. This effect is expected to be phonon mode specific and would require a case by case study of the different phonon modes. Since the influence of strain appears to be non-uniform between phonon modes for both the pDOS and strength of interaction, further study and calculations of the influence of strain on the phonon-phonon strength of interaction and scattering rates are needed to determine the full effect of mechanical strain on the thermal behavior of CNTs.

IV. CONCLUSIONS

Supercell theory and molecular mechanics were successfully used to calculate the phonon dispersion of a strained (10, 10) CNT. The results show a clear downshift in longitudinal phonon energy for increasing tensile strain. This downshift is believed to be responsible for an increase in both the electron-phonon scattering rates in strained CNTs. This increase offers an additional explanation to the deterioration of electrical properties of CNTs under mechanical strain on top of the change of bonding type proposed by Ref. 23. This phonon quantization tuning through strain is of great importance for the design of flexible electronic devices, in which electrical behavior could be to some extent controlled by an applied deformation. Further study is needed to properly quantify the increase in both the electron-phonon and the phonon-phonon scattering rates, and understand their influences on the electrical properties of strained CNTs. Such studies are currently under way in our laboratory.

ACKNOWLEDGMENTS

This project has been funded by the US Navy Office of Naval Research Advanced Electrical Power Systems Program under P. Cho.

[1]P. G. Collins, M. Hersam, M. Arnold, R. Martel, and P. Avouris, Phys. Rev. Lett. **86**, 3128 (2001).
[2]Z. Shengli, X. Minggang, Z. Shumin, X. Tao, and Z. Erhu, Phys. Rev. B **68**, 75415 (2003).
[3]O. Zhun-Yong and E. Pop, Phys. Rev. B **81**, 155408 (2010).
[4]W. Wei, Y. Liu, Y. Wei, K. Jiang, L.-M. Peng, and S. Fan, Nano Lett. **7**, 64 (2007).
[5]T. Ragab and C. Basaran, J. Appl. Phys. **106**, 063705 (2009).
[6]A. Akturk, N. Goldsman, and G. Pennington, J. Appl. Phys. **102**, 073720 (2007).
[7]Y. Cheng, S. Lu, H. Zhang, C. V. Varanasi, and J. Liu, Nano Lett. **12**, 4206 (2012).
[8]T.-K. Hong, D. W. Lee, H. J. Choi, H. S. Shin, and B.-S. Kim, ACS Nano **4**, 3861 (2010).
[9]C. Kyoung-Yong, O. Youngseok, R. Jonghyun, A. Jong-Hyun, K. Young-Jin, C. Hyouk Ryeol, and B. Seunghyun, Nat. Nanotechnol. **5**, 853 (2010).
[10]I. Lahiri, V. P. Verma, and C. Wonbong, Carbon **49**, 1614 (2011).
[11]J. Liang, Y. Chen, Y. Xu, Z. Liu, L. Zhang, X. Zhao, X. Zhang, J. Tian, Y. Huang, Y. Ma, and F. Li, ACS Appl. Mater. Interfaces **2**, 3310 (2010).
[12]X. Lu, H. Dou, B. Gao, C. Yuan, S. Yang, L. Hao, L. Shen, and X. Zhang, Electrochim. Acta **56**, 5115 (2011).
[13]T. Ito, K. Nishidate, M. Baba, and M. Hasegawa, Surf. Sci. **514**, 222 (2002).
[14]Y. Liu and H. Jie, Phys. Rev. Lett. **85**, 154 (2000).
[15]B. Gao, L. Jiang, X. Ling, J. Zhang, and Z. Liu, J. Phys. Chem. C **112**, 20123 (2008).
[16]T. Ando, J. Phys. Soc. Jpn. **74**, 777 (2005).
[17]P. Gautreau, T. Ragab, and C. Basaran, J. Appl. Phys. **112**, 103527 (2012).
[18]A. Verma, M. Z. Kauser, and P. P. Ruden, J. Appl. Phys. **97**, 114319 (2005).
[19]P. Gautreau, T. Ragab, and C. Basaran, Carbon **57**, 59 (2013).
[20]H. Ishii, N. Kobayashi, and K. Hirose, J. Vac. Sci. Technol., B **27**, 882 (2009).
[21]G. Pennington and N. Goldsman, Phys. Rev. B **68**, 45426 (2003).
[22]C. Yi-Ray and I. W. Cheng, Carbon **45**, 1636 (2007).
[23]T. W. Tombler, Z. Chongwu, L. Alxseyev, K. Jing, D. Hongjie, L. Lei, C. S. Jayanthi, T. Meijie, and W. Shi-Yu, Nature **405**, 769 (2000).
[24]W. Frank, C. Elsasser, and M. Fahnle, Phys. Rev. Lett. **74**, 1791 (1995).
[25]Y. Lin-Hui, L. Bang-Gui, W. Ding-Sheng, and R. Han, Phys. Rev. B **69**, 235409 (2004).
[26]Y. Wei, P. Liu, K. Jiang, L. Liu, and S. Fan, Appl. Phys. Lett. **93**, 023118 (2008).
[27]D. W. Brenner, O. A. Shenderova, J. A. Harrison, S. J. Stuart, B. Ni, and S. B. Sinnott, J. Phys.: Condens. Matter **14**, 783 (2002).
[28]R. A. Jishi, M. S. Dresselhaus, and G. Dresselhaus, Phys. Rev. B **48**, 11385 (1993).
[29]T. Ragab and C. Basaran, Comput. Mater. Sci. **46**, 1135 (2009).
[30]J. Maultzsch, S. Reich, C. Thomsen, E. Dobardzic, I. Milosevic, and M. Damnjanovic, Solid State Commun. **121**, 471 (2002).
[31]G. Samsonidze, R. Saito, A. Jorio, M. Pimenta, A. S. Filho, A. Gruneis, G. Dresselhaus, and M. Dresselhaus, J. Nanosci. Nanotechnol. **3**, 431 (2003).
[32]E. B. Barros, A. Jorio, G. G. Samsonidze, R. B. Capaz, A. G. S. Filho, J. M. Filho, G. Dresselhaus, and M. S. Dresselhaus, Phys. Rep. **431**, 261 (2006).
[33]J. Kurti and V. Zolyomi, AIP Conf. Proc. **723**, 377 (2004).
[34]V. Zolyomi and J. Kurti, Phys. Rev. B **70**, 085403 (2004).
[35]G. Pennington, S. J. Kilpatrick, and A. E. Wickenden, Appl. Phys. Lett. **93**, 093110 (2008).
[36]J. W. Lu, W. L. Wang, K. J. Liao, and B. Y. Wan, in *Proceedings of Fifth International Conference on New Theories, Discoveries and Applications of Superconductors and Related Materials (New3SC-5), 11-16 June 2004* (World Scientific, Singapore, 2004), Vol. 19, pp. 627–629.
[37]J. Hoon-Sik, L. Yun-Hee, N. Ho-Jun, and N. Seung Hoon, J. Appl. Phys. **104**, 114304 (2008).
[38]G. P. Srivastava, *The Physics of Phonons* (Taylor & Francis Group, New York, 1990).
[39]S. P. Hepplestone and G. P. Srivastava, Phys. Rev. B **74**, 165420 (2006).